ОБЪЕДИНЕННЫЙ
ИНСТИТУТ
ЯДЕРНЫХ
ИССЛЕДОВАНИЙ
Дубна

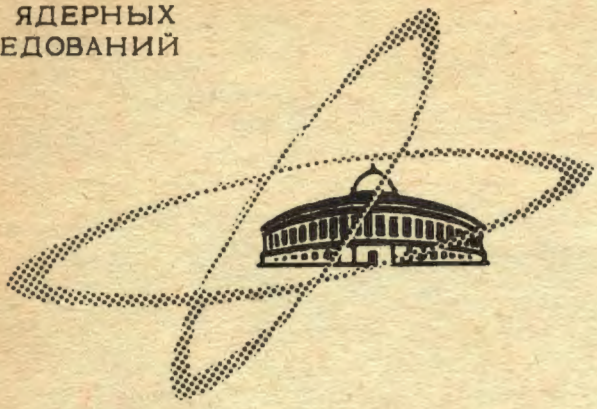

E1- 3708

J.Čech, Z.Janout, F.Lehar. Z.Málek

ELASTIC SCATTERING OF 660 MeV PROTONS ON LMN CRYSTALS

1968

E1- 3708

J.Čech, Z.Janout, F.Lehar. Z.Málek

ELASTIC SCATTERING OF 660 MeV PROTONS ON LMN CRYSTALS

Submitted to Nucl.Instr. and Methods

Чех Я., Яноут З., Легар Ф., Малек З. E1-3708

Упругое рассеяние протонов 660 Мэв на кристалле.

Изучается упругое и квазиупругое рассеяние протонов с энергией 660 Мэв на мишенях: кристалле LMN ($La_2Mg_3(NO_3)_{12} \times 24\,H_2O$) , эквивалентной безводородной мишени из $Ba(NO_3)_2$ (36,37 %) , MgO (63,63 %) и политена CH_2 . Результаты можно использовать для планирования экспериментов по N – N -рассеянию на протонной поляризованной мишени из LMN .

Препринт Объединенного института ядерных исследований.
Дубна, 1968.

Čech J., Janout Z., Lehar F., Málek Z. E1-3708

Elastic Scattering of 660 MeV Protons on LMN Crystals

Elastic and quasielastic 660 MeV proton scattering on various targets has been investigated. Crystal LMN ($La_2Mg_3(NO_3)_{12} \times 24\,H_2O$), the equivalent dummy target consisting of $Ba(NO_3)_2$ (36.37 %) and MgO (63.63 %) and polythene CH_2 were used as targets. The results can be used for the planning of the nucleon-nucleon scattering experiments on a proton polarized target.

**Preprint. Joint Institute for Nuclear Research.
Dubna, 1968**

1. Introduction

The investigation of the elastic scattering of protons on LMN ($La_2Mg_3(NO_3)_{12} \times 24H_2O$) [*] crystals, used as proton polarized targets, needs the separation of p – p scattering on a background of other processes. From the formula it follows, that the LMN crystal contains only 3.168% of free hydrogen (in crystaline water) which can be polarized by the dynamic method [1,2].

The scattered proton and the corresponding recoil proton are detected simultaneously in order to separate the p – p elastic and quasielastic scattering processes from all other events.

The aim of the present investigation is to determine the amount of quasielastic events, using a hydrogenless target (a dummy target-DT), with the same number of the bound protons as LMN. The ratios of the elastic p – p scattering on the LMN crystal and on a polythene target CH_2 are determined with account of the quasielastic processes on DT and carbon C, respectively.

Since the conditions of the experiments with CH_2 are well

[*] The crystal contains also about 1 % of neodymium even isotopes.

known, the comparison of the CH_2 target and the LMN crystal, carried out in the present investigation, make it possible planning of experiments on the proton polarized target (PPT) with the LMN crystal.

2. Targets

Targets of LMN, DT, CH_2 and C as well as the copper foil, in which the targets were packed, were used in the experiments. The weights and the sizes of the targets are given in Table 1.

Special attention was paid to the preparation of the DT. The consistence of the DT and the LMN target is given in Table 2. The components of the DT $Ba(NO_3)_2$ (36.37 %) and MgO (63.63 %) contained about 2 % of water and organic admixtures *). We got rid of these by anealing MgO at 800°C and $Ba(NO_3)_2$ at 300°C (the melting point 592°C). The changes of the $Ba(NO_3)_2$ weight during a long time heating were nearly negligible. The obtained mixture has four times lower density than LMN. The powder must be pressed at about 3000 kg/cm^2 in order to obtain the same density as LMN ($2g/cm^3$). A special mould is necessary for such a high pressure. For this reason a mould suitable for pressing about 100 DT samples was constructed (see Fig.1) The obtained targets it is possible to machine to the necessary size with the help of emery. After a second anealing at 300°C for 10 hours, the samples were packed in a Cu foil, since

*) *In the Rutherford High Energy Laboratory a mixture of $BaCO_3$ (26.2 %) and MgO (7.8 %) with teflon powder (66 %) was used as the DT. The density of this heat pressed mixture is greater than that of LMN, the required average density is made by stacking together a large number of thin plates (perpendicular to beam direction) leaving gaps between the layers* [3].

at 60 % air moisture their surface adsorb water with the initial velocity of about 0.5 mg/cm^2 min.

3. *Experimental Equipment*

The scheme of experiment is shown in Fig.2. The 660 MeV proton beam from the Dubna synchrocyclotron transmitted through a system of colimators is scattered on the investigated target. The beam average intensity was 10^8 protons (sec.cm^2.) The scattered and recoil protons were detected by two scintillation counter telescopes A.B. respectively (Fig.2). Plastic scintillators 50 x 25 x 5 mm^3 were used in the detectors. The angular resolution of the telescopes was $\Delta\theta = \pm 0.75^\circ$ and $\Delta\phi = \pm 1.75^\circ$, where ϕ is the azimuthal angle.

The counters of each telescope were connected in triple coincidence circuits C_1, C_2 with the time resolution of 5 x 10^{-9} sec. The output pulses from the triple coincidence circuit were simultaneously transmitted to the double coincidence circuit C_3 and C_4. The C_4 registered the background of random coincidences, whereas C_3 registered the elastic and quasielastic p-p scattering events together with the background.

At two angles of 50° and 90° c.m.s. the measurements on the other experimental equipment in usual condition for a PPT were performed. This equipment is described in ref./4/. The LMN crystal of size 20x30x20 mm^3, inside the cryostat. and DT. CH_2 and C targets were used. These targets of the same sizes were put inside the model of cryostat during the measurements.

The primary proton beam was detected by the two monitors M_1 and M_2 (Fig.2).

1. Measurements and Data Processing

The measurements were performed for six scattering angles in the region $\theta = 30^{\circ}-90^{\circ}$(c.m.s.). The telescope A always determined the scattering angle, telescope B detected the recoil particles in the vicinity of the conjugate angle x_0 (lab. syst.). The scattering was successively performed on the LMN, DT, CH_2 and C targets and on the Cu foil. The counting rate $N_{ef+b}(\theta, x)$ for the considered effect together with the random coincidence background $N_b(\theta, x)$ and N_m for the monitor M_2 were determined simultaneously. Here, x is the laboratory angle between the telescope B and the initial direction of the beam.

The dependences the number of pulses N on the angle (θ fixed) were approximated by the functions

$$f_1(\theta, x) = \frac{a}{b^2 + (x - x_0)^2} + \sum_{i=0}^{a} c_i x^i \quad , \tag{1}$$

$$f_2(\theta, x) = \sum_{k=0}^{M} d_k x^k \quad . \tag{2}$$

The function $f_1(\theta, x)$ approximates the dependence of effect togehter with the background N_{ef+b} on x, the function $f_2(\theta, x)$ approximates that of the background alone. The quantities x_0, a, b, c_i, d_k are variable parameters and were determined together with their errors using the least squares method. The number of variable parameters was chosen according to the χ^2 criterion in such a manner, that $\chi^2/\bar{\chi}^2$ is not descreased when a further coefficient is added.

On the basis of calculated values $f_1(\theta, x_0)$ and $f_2(\theta, x_0)$ for all the targets, we can determine the following ratios:

$$\frac{N_{LMN} - N_{DT}}{N_{CH_2} - N_C} = \frac{[f_1(\theta, x_0) - f_2(\theta, x_0)]_{LMN} - [f_1(\theta, x_0) - f_2(\theta, x_0)]_{DT}}{[f_1(\theta, x_0) - f_2(\theta, x_0)]_{CH_2} - [f_1(\theta, x_0) - f_2(\theta, x_0)]_C} \quad (3)$$

$$\frac{N_C}{N_{CH_2}} = \frac{[f_1(\theta, x_0) - f_2(\theta, x_0)]_C}{[f_1(\theta, x_0) - f_2(\theta, x_0)]_{CH_2}} \quad (4)$$

$$\frac{N_{LMN} - N_{DT}}{N_{LMN}} = \frac{[f_1(\theta, x_0) - f_2(\theta, x_0)]_{LMN} - [f_1(\theta, x_0) - f_2(\theta, x_0)]_{DT}}{[f_1(\theta, x_0) - f_2(\theta, x_0)]_{LMN}} \quad (5)$$

$$\frac{N_{DT}}{N_{LMN}} = \frac{[f_1(\theta, x_0) - f_2(\theta, x_0)]_{DT}}{[f_1(\theta, x_0) - f_2(\theta, x_0)]_{LMN}} \quad (6)$$

It was checked experimentally that in our case the $p - p$ scattering on the Cu foil is negligible smaller than 0.1 % of measured effect on LMN crystal.

5. *Results*

The values calculated according to formulae (3)–(6) for the elastic and quasielastic effect of $p - p$ scattering on CH_2 and LMN are given in Tab.3. The errors of this ratios represent the mean squared deviations. All the measured data are normalized

to the same counting rates of the monitor and to the same number of bound protons in CH_2 , C and LMN, DT, respectively.

The dependence of $f_1(90°, x)$ and $f_2(90°, x)$ on the angle x at $\theta = 90^\circ$ c.m.s. for LMN, CH_2 and DT are shown in Fig.3. The analogous dependences for the angles 75° and 40° c,m.s. are shown in Fig.4 and 5. The corridor of errors has been calculated on the basis of the error matrix.

The same ratios measured at 50° and 90° c.m.s. in the dependence of the target thikness are given in Table 4. The asterisks denote the measurements, performed in conditions of PPT.

The dependences $f_1 - f_2$ at 90° for the LMN crystal and DT on x in PPT conditions are shown in Fig.6a,b. For comparison the function $f_1 - f_2$ for CH_2 and C of the same weights are plotted in Fig.6c,d. In all figures, the coordinate system with $x_0 = 0$ is used.

It follows from Tables 3 and 4 that the ratio of elastic $p - p$ scattering events in LMN and CH_2 is always smaller than that of the number of free hydrogen nuclei for equal weights of the samples (this ratio is equal to 22.01 %) The geometrical conditions were equal since the sizes of all targets were the same and all the results were reduced to the same numbers of bound protons. This effect may be due to different multiple scatterings, different absorptions and different scatterings on complex nuclei in LMN and CH_2 . This difference increases as the energy of the recoil particle decreases and the thickness of the LMN target increases.

For scattering angles smaller than 30° c.m.s., when the recoil proton is emitted at a large angle and its energy is small, the ratio of the background to the measured effect increases significantly, so that the accurancy of the measurements decreases (Tables 5 and 6). The number of quasielastic $p - p$ scattering processes also increases, as can be seen from Table 3 and Fig.5.

It follows from the above discussion, that for angles smaller than 30°, it is necessary to reduce the thickness of LMN polarized targets considerably. It is very desirable to obtain a PPT with a higher relative hydrogen content, even if this would mean a decrease in the magnitude of the polarization.

The LMN target was many times irradiated (200 hours with the proton beam of intensity about 10^{8} protons/sec.cm^{2}. taken in high vacuum and was cooled down to 1°K .

The chemical analysis was made in which it can be determined, how the contain of water changes. Two samples of LMN are analysed one of them was irradiated, the second one was not used yet*).

Since the LMN crystal was not hermeticaly packed, and his surface is hydroscopic, the surface as the internal part (which gives a main scattering effect) was analysed separately. The results are presented in Table 7. The mean squared error is equal to 0.1%.

From the Table it follows that LMN crystal during a long time irradiations, losed a part of crystaline water and his consistence changed. On the other hand his surface absorbes a moisture from air and in view of this each crystal must be taken in exicator or hermetically packed.

In conclusion the authors express their deep gratitude to N.Malkova for constructing the high-pressure mould , I.Dudova for the chemical analysis of LMN crystal, M.Borghini, Yu.M.Kazarinov and P.Winternitz for helpful discussions, E.Dudova , J.Fingerova, R.Tichy and J.Sacha for help in the work.

*) *In all the measuremenls, discussed above, the non-irradiated LMN crystals were used.*

References

1. A.Abragam, M.Borghini. Progress in Low Temperature Physics, ed. by C.J.Gorter, Amsterodam, Vol. IV, 1964, p.384.
2. C.J.Jeffries, Dynamic Nuclear Orientation, Interscience Publishers, New York 1963.
3. H.H.Atkinson. Proceedings of the International Conference on Polarized Targets and Ion Sources. Saclay 1966, p.41.
4. Yu.M. Kazarinov, Rev. Mod. Phys. 39, 509 (1967).

Received by Publishing Department
on February 13, 1968.

Table 1

Targets		Size in [mm]	Weight in gr.	g/cm^2
1.	LMN	22 x 15	11.7379	3.089
2.	LMN	—	—	1.358
3.	LMN	20 x 30 x 20	24.00	4.00
4.	LMN	20 x 30 x 22	26.40	4.00
5.	DT	22 x 15	11.6099	3.055
6.	DT	20 x 20 x 30	23.0361	3.839
7.	CH_2	30 x 6	4.239	0.600
8.	CH_2	20.5 x 15	4.6369	1.405
9.	CH_2	10 x 20 x 30	5.70	0.95
10.	CH_2	30 x 13.4	8.730	1.236
11.	CH_2	20 x 30 x 20	12.0085	2.001
12.	C	22 x 15	11.8385	—
13.	C	20 x 30 x 20	22.3475	—
14.	Cu	23 x 16	2.6964	—

Table 2

The structure of dummy target and LMN crystal.

Element	Z	A_i	$n_i A_i$	$\frac{n_i A_i}{A}$	Weight in gr.
Dummy target					
Ba	56	137.36	279.75	0.188	2.30
Mg	12	24.32	356.29	0.240	2.94
N	7	14.01	85.51	0.058	0.70
O	8	16.00	762.24	0.514	6.28
			A = 1483.79	1.000	12.22
LMN target: $La_2 Mg_3 NO_3 12 \cdot 24H_2O$					
La	57	138.92	277.84	0.1819	2.193
Mg	12	24.32	72.96	0.0478	0.574
N	7	14.01	168.12	0.1101	1.321
H	1	1.008	48.38	0.0317	0.380
O	8	16.00	960.00	0.6285	7.542
			A = 1527.30	1.0000	12.000

Table 3

The ratios of the p-p elastic and quasiclastic effects for various scattering angles ϑ. The targets of size ϕ 22x15 were used.

ϑ c.m.s.	$\frac{N_{LMN} - N_{OT}}{N_{CH_2} - N_C}$	$\frac{N_C}{N_{CH_2}}$	$\frac{N_{LMN} - N_{OT}}{N_{LMN}}$	$\frac{N_{OT}}{N_{LMN}}$
90°	19.41 ± 0.37	1.89 ± 0.34	93.31 ± 2.25	6.69 ± 0.92
75°	15.50 ± 0.39	—	91.87 ± 2.75	8.13 ± 0.97
60°	14.84 ± 0.44	1.57 ± 0.20	92.74 ± 2.95	7.26 ± 0.99
50°	13.00 ± 0.27	1.93 ± 0.23	92.58 ± 2.23	7.42 ± 0.76
40°	10.44 ± 0.47	—	84.04 ± 4.60	15.94 ± 1.98
35°	—	3.48 ± 0.54	—	—
30°	11.4 ± 2.7	—	77.8 ± 22.0	22.20 ± 53.36

Table 4

The ratios of the p-p elastic and quasielastic scattering effects for the targets of various thickness.

ϑ c.m.s.	w [g/cm²]	d [cm]	$\frac{N_{LMN} - N_{OT}}{N_{CH_2} - N_C}$	$\frac{N_C}{N_{CH_2}}$	$\frac{N_{LMN} - N_{OT}}{N_{LMN}}$	$\frac{N_{OT}}{N_{LMN}}$
90°	4.0*)	2.0	13.90±0.35	1.32±0.08	92.34±1.13	7.26±0.92
90°	3.09	1.5	19.41±0.37	1.89±0.34	93.31±2.25	6.69±0.92
90°	1.36	0.79	19.62±0.40		94.11±2.48	5.89±0.90
50°	4.0*)	2.0	15.01±0.35	2.84±0.47	90.13±1.10	9.87±0.86
50°	3.09	1.5	13.00±0.27	1.93±0.23	92.58±2.23	7.42±0.76

*) The data measured in useful conditions of the PPT.

Table 5

The ratios of the p-p scattering effect to that together with the background of random coincidences as a function of the beam intensity /in relative units/.

$\frac{f_1(90°, x_0)}{f_1(90°, x_0) + f_2(90°, x_0)}$			Beam Intensity
CH_2 (w = 0.95g/cm^2)	LiN (w = 4.0g/cm^2)	LiN (w = 1.35g/cm^2)	
99.91 ± 1.91	95.71 ± 2.68		100
99.87 ± 2.56	90.3 ± 4.6	99.1 ± 4.7	122
98.5 ± 1.6	85.5 ± 4.7		194
97.9 ± 2.4	71.9 ± 3.6		294
95.5 ± 3.2	48.59 ± 0.82		569

Table 6

The ratios of the p-p scattering effect to that together with the background of random coincidences as function of the scattering angle c.m.s. The targets of size 22 x 15 were used.

ϑ c.m.s.	$\frac{f_1(90°, x_0)}{f_1(90°, x_0) + f_2(90°, x_0)}$		
	CH_2	LiN	DT
90°	98.7 ± 2.1	91.3 ± 2.3	40.1 ± 7.6
90°	96.3 ± 1.9	87.3 ± 2.2	39.9 ± 4.1
75°	98.6 ± 1.4	87.3 ± 2.1	37.7 ± 4.0
60°	99.3 ± 2.3	92.2 ± 2.8	39.3 ± 5.7
50°	99.0 ± 1.9	91.2 ± 2.7	54.5 ± 4.7
50°	97.9 ± 1.8	97.4 ± 2.5	21.0 ± 4.7
40°	95.4 ± 2.7	63.9 ± 4.0	23.3 ± 5.0
40°	95.5 ± 2.4	73.9 ± 4.0	32.4 ± 5.1
30°	44.6 ± 2.3	25.4 ± 3.6	1.8 ± 4.2

Table 7

The content of crystaline water and of hydrogen in LMN crystal before and after irradiation. Theoretical values are 28.3084 % of H_2O and 3.1677 % of H .

	Internal Part		Surface	
	H_2O %	H %	H_2O %	H %
Before irradiation	29.95	3.32	34.98	3.84
After irradiation	25.04	2.78	31.81	3.54

The accuracy of measurement is equal to 0.1 % .

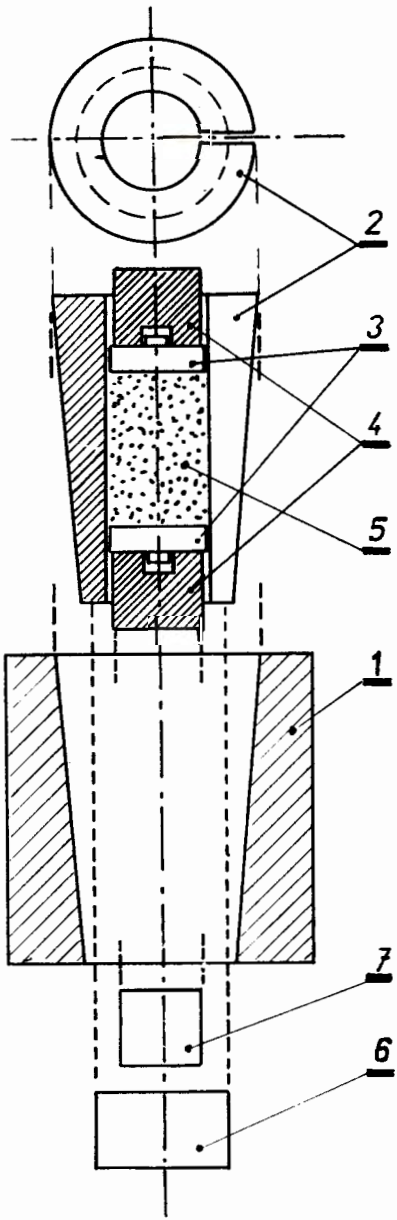

Fig.1 High pressure mould for DT fabrication, 1-steel carcass designed for a high static pressure, 2,3-cone matrix and two punches made of hardened steel, 4-buffers transmiting the pressure from the external press to the mixture pressed (5), 6,7-steel pistons forcing out the cone matrix and fabricated samples, respectively.

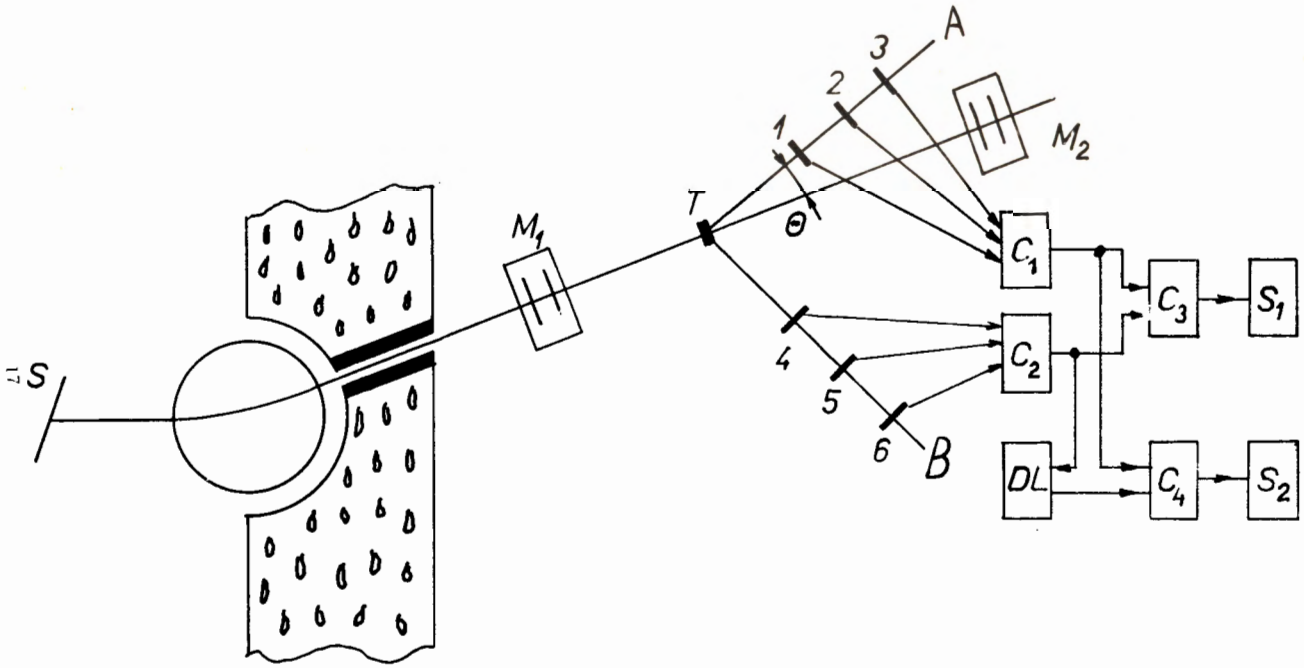

Fig.2 Experimental arrangement, S-synchrocyclotron, A,B-scintillation counter telescopes, M_1,M_2-monitors, C_1, C_2-triple coincidence circuits, C_3,C_4-double coincidence circuits, DL-delay line., S_1,S_2-scalers.

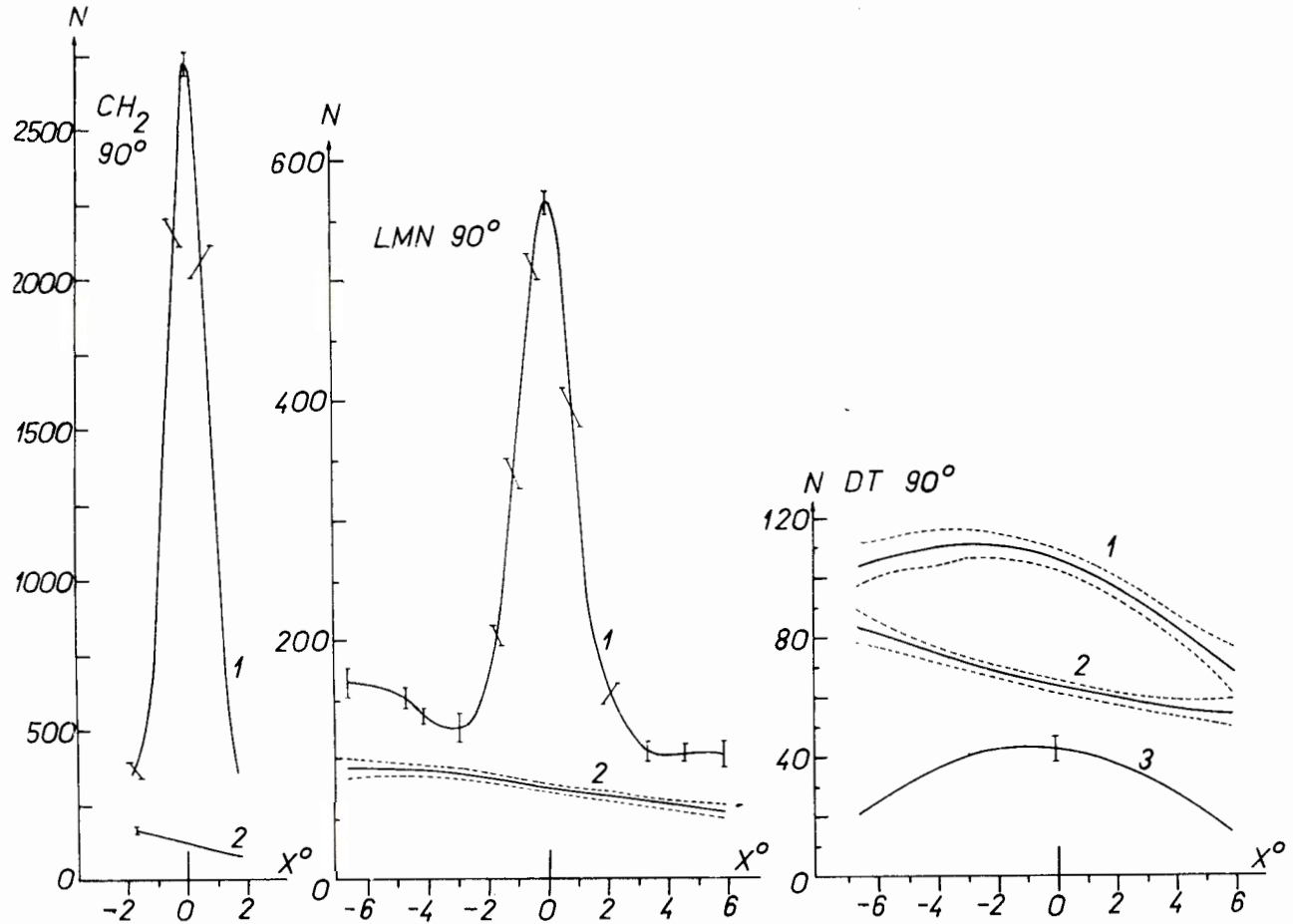

Fig.3. The dependence of the counting rates $f_1(90°, x)$ (curve 1), $f_2(90°, x)$ (curve 2) and $f_1(90°, x) - f_2(90°, x)$ (curve 3) on the angle x. The coordinate system with $x_0 = 0$ is used.

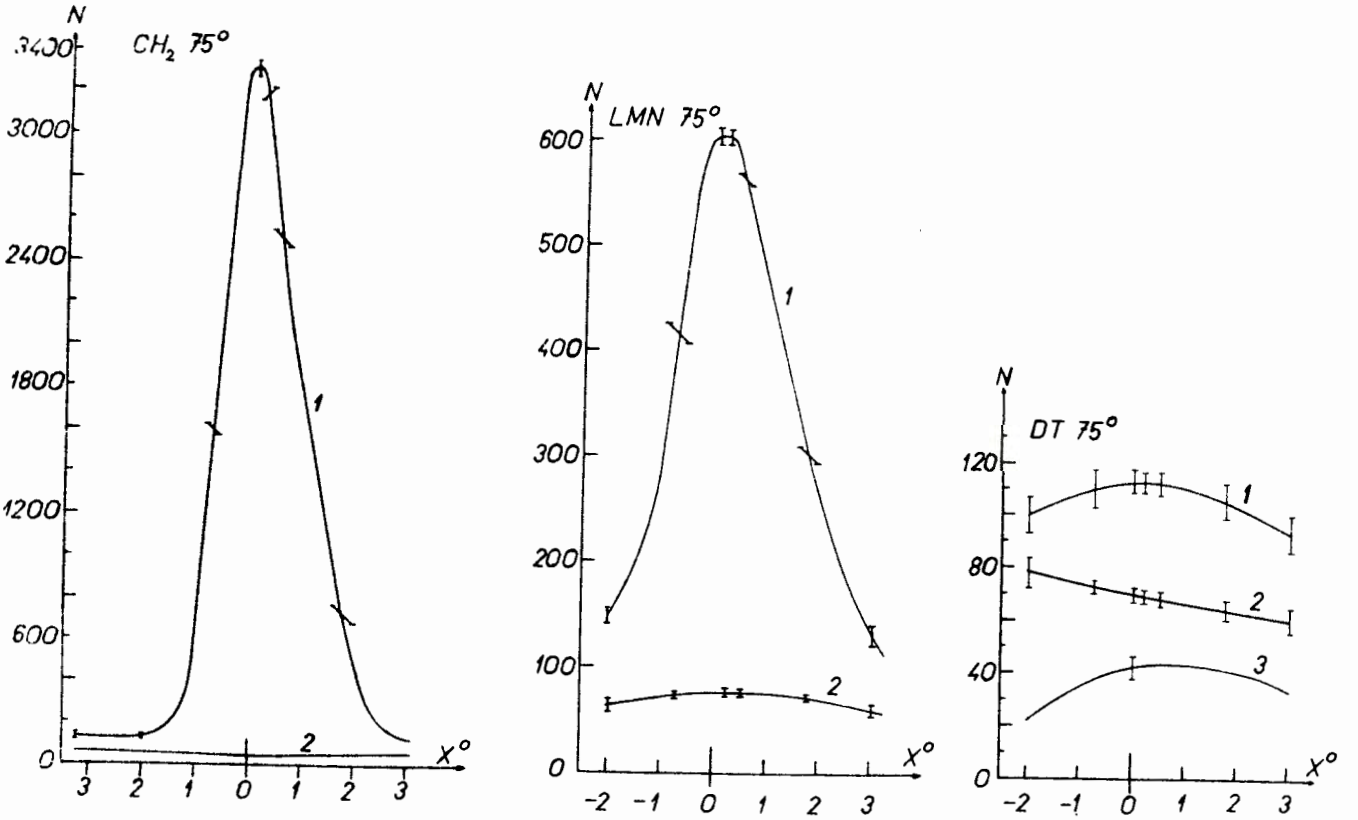

Fig.4. The dependence of the counting rates $f_1(75^\circ, x)$ (curve 1), $f_2(75^\circ, x)$ (curve 2) and $f_1(75^\circ, x) - f_2(75^\circ, x)$ (curve 3) on x ($x_c = 0$)

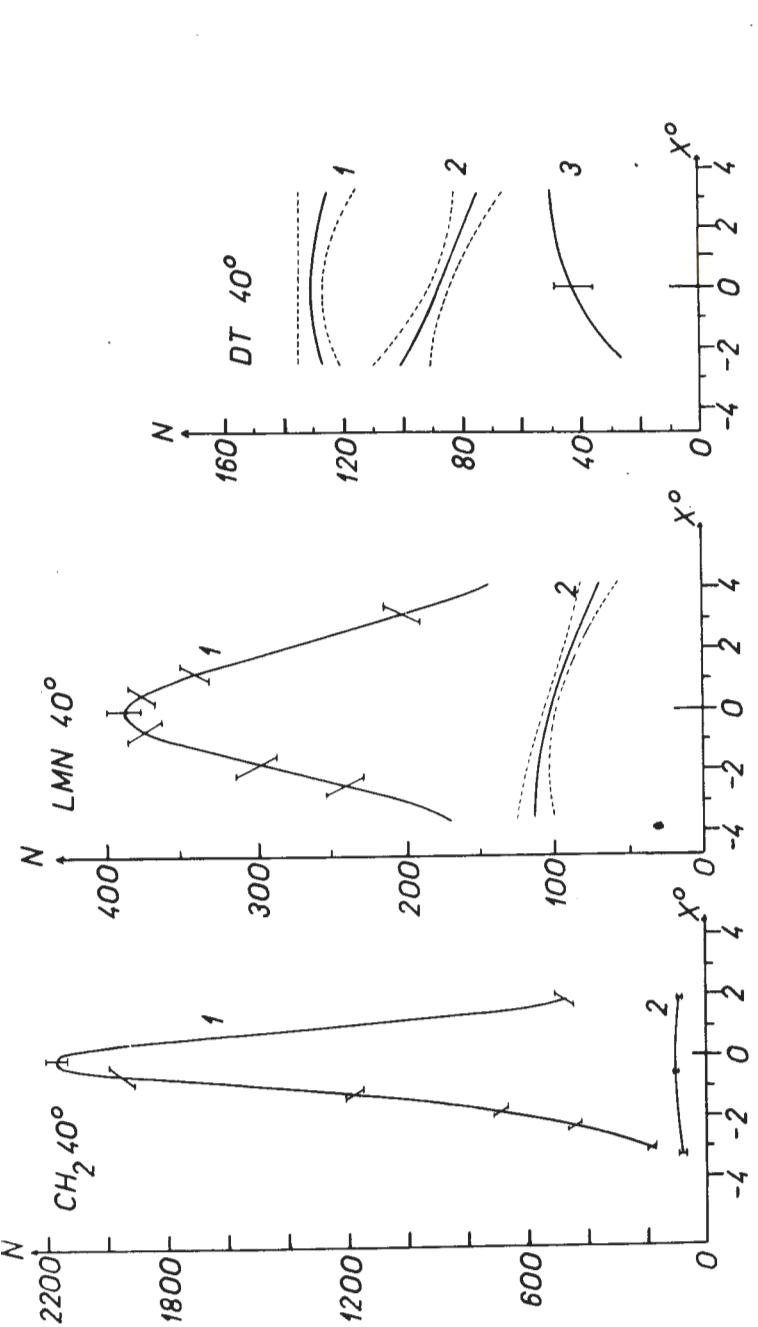

Fig.5 The dependence of $f_1(40°, x)$ (curve 1), $f_2(40°, x)$ (curve2), and $f_1(40°, x) - f_2(40°, x)$ (curve 3) on x ($x_0 = 0$).

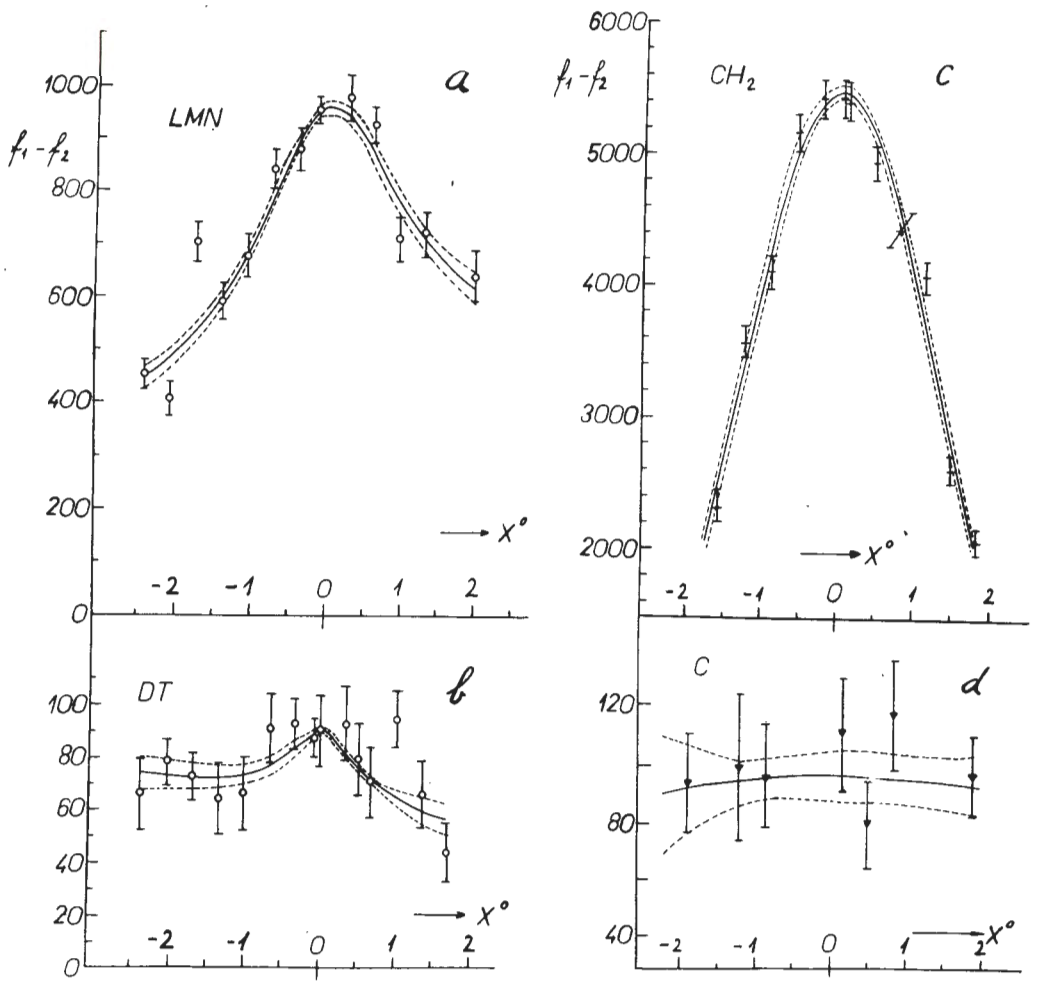

Fig.6 The dependences of $f_1 - f_2$ at $\theta = 90^\circ$ on x in PPT conditions for various targets.